

SCIENTIFIC REPORTS

OPEN

Cytochrome *bd* Displays Significant Quinol Peroxidase Activity

Sinan Al-Attar^{1,†}, Yuanjie Yu¹, Martijn Pinkse¹, Jo Hoeseer², Thorsten Friedrich², Dirk Bald³ & Simon de Vries^{1,5}

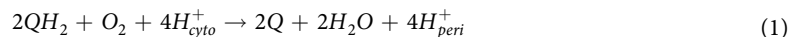
Received: 23 March 2016

Accepted: 23 May 2016

Published: 09 June 2016

Cytochrome *bd* is a prokaryotic terminal oxidase that catalyses the electrogenic reduction of oxygen to water using ubiquinol as electron donor. Cytochrome *bd* is a tri-haem integral membrane enzyme carrying a low-spin haem *b*₅₅₈ and two high-spin haems: *b*₅₉₅ and *d*. Here we show that besides its oxidase activity, cytochrome *bd* from *Escherichia coli* is a genuine quinol peroxidase (QPO) that reduces hydrogen peroxide to water. The highly active and pure enzyme preparation used in this study did not display the catalase activity recently reported for *E. coli* cytochrome *bd*. To our knowledge, cytochrome *bd* is the first membrane-bound quinol peroxidase detected in *E. coli*. The observation that cytochrome *bd* is a quinol peroxidase, can provide a biochemical basis for its role in detoxification of hydrogen peroxide and may explain the frequent findings reported in the literature that indicate increased sensitivity to hydrogen peroxide and decreased virulence in mutants that lack the enzyme.

Cytochrome *bd* is an integral membrane terminal oxidase that uses ubiquinol as the physiological electron donor for catalysing the reduction of molecular oxygen to water^{1–4}. This strictly prokaryotic oxidase is found in many bacterial pathogens^{5–14} and contributes to the formation of the proton motive force by vectorial charge transfer without actual proton pumping^{15–19}. Protons (H⁺_{cyto}) are taken up at the cytoplasmic side of the membrane for water formation whereas quinol (QH₂) oxidation leads to proton (H⁺_{peri}) release at the periplasmic side (Eq. 1).



The bioenergetic efficiency of cytochrome *bd* is half that of the oxygen-reducing cytochrome oxidases, which in addition to consuming chemical protons also pump protons across the membrane (reviewed in²⁰).

Cytochrome *bd* is a tri-haem protein carrying haem *b*₅₅₈ which is ligated by His186 and Met393 (*Escherichia coli* numbering), haem *b*₅₉₅ ligated by His19 and Glu99, and haem *d* ligated by Glu445²¹. Haems *b*₅₉₅ and *d* are proposed to constitute a functional binuclear site, similar to the binuclear haem-Cu_B site in haem-copper oxidases where the oxygen chemistry takes place^{20,22–27} (but see²¹). An important mechanistic feature in both classes of enzymes is that the reduction of oxygen occurs in a concerted 4-electron redox reaction preventing the formation of reactive oxygen species (ROS): superoxide (O₂^{•−}), hydrogen peroxide (H₂O₂) and the hydroxyl radical²⁸.

ROS are produced endogenously when molecular oxygen is partially reduced to superoxide and H₂O₂ by redox enzymes, especially flavoenzymes, including the respiratory chain Complex I^{29–34}. Two superoxide anions dismutate to H₂O₂ and O₂ in the cell either spontaneously or catalysed enzymatically by superoxide dismutase (SOD). When H₂O₂ is reduced by cellular Fe²⁺ through Fenton chemistry, hydroxyl radicals are produced leading to a wide spectrum of damage to biological molecules^{35,36}. In addition to lipids and DNA, protein targets of ROS, which lead to enzyme inactivation, include solvent-exposed Fe-S clusters of dehydratases among which aconitases and fumarases and the Isc system responsible for Fe-S cluster synthesis^{37,38}. Cells not only have to cope with endogenous ROS. Microorganisms must also detoxify ROS produced extracellularly by competing microorganisms and in the case of pathogenic microorganisms by host immune systems^{39–41}.

In order to protect themselves from oxidative damage, prokaryotes express different ROS scavenging enzymes and employ low-molecular weight agents such as ascorbate and glutathione^{36,42,43}. In addition to SOD, *E. coli* synthesizes a number of specific cytoplasmic H₂O₂-scavenging enzymes: the catalases KatG and KatE³⁶;

¹Department of Biotechnology, Delft University of Technology, The Netherlands. ²Institut für Biochemie, Albert-Ludwigs-Universität Freiburg, Albertstr 21, 79014 Freiburg i. Br., Germany. ³Department of Molecular Cell Biology, AIMMS, Faculty of Earth- and Life Sciences, VU University Amsterdam, Amsterdam, The Netherlands. [†]Present address: Aix-Marseille Université, CNRS, Unité de Bioénergétique et Ingénierie des Protéines (UMR7281), Institut de Microbiologie de la Méditerranée, 13009 Marseille, France. [§]Deceased. Correspondence and requests for materials should be addressed to S.A.-A. (email: salattar@imm.cnrs.fr)

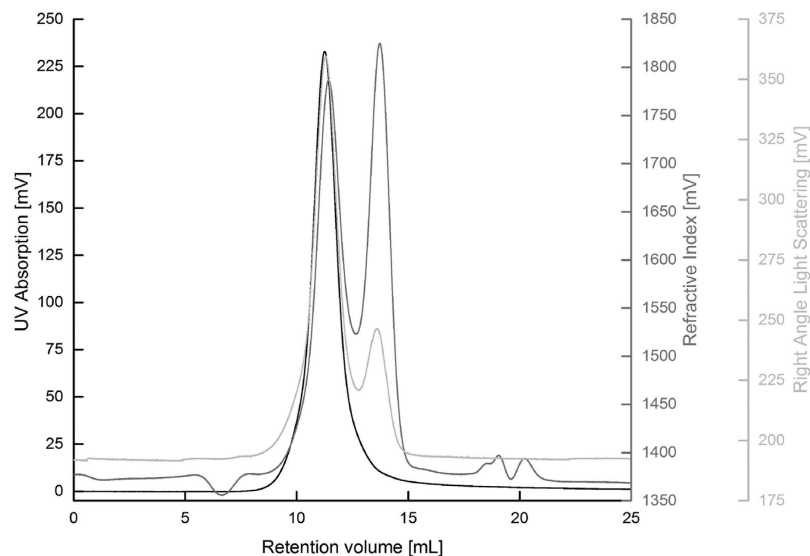


Figure 1. Analytical chromatography of purified cytochrome *bd*. Purified cytochrome *bd* was subjected to analytical gel filtration chromatography. UV absorption at 280 nm is shown in black, refractive index and right angle light scattering are shown in gray and light gray, respectively. A monodisperse protein peak was detected at an elution volume of 11.3 mL, corresponding to a mass of approximately 470 kDa. A second non-protein peak was detected at 13.7 mL, corresponding to a mass of approximately 70 kDa.

NADH-dependent alkyl hydroperoxide reductase (Ahp)⁴⁴, glutathione peroxidase (GPX)^{45,46} and thiol peroxidase^{47,48}. In aerobically growing *E. coli* cells, the main H₂O₂ scavengers are KatG, KatE and Ahp⁴².

Cytochrome *bd* has been proposed to confer protection to oxygen-sensitive enzymes and to help protect the cell from nitrosative and ROS stresses^{7,49–55}. It was shown that cytochrome *bd* knockouts were highly sensitive to hydrogen peroxide and showed increased levels of endogenous ROS^{6,54,56,57}, including ROS resulting from antibiotic-induced stress^{58,59}. Cytochrome *bd* knockouts in *Mycobacteria* were highly susceptible to drugs acting on oxidative phosphorylation^{58,60,61}. In addition, numerous studies concerning pathogenic bacteria indicated that lack of a functioning cytochrome *bd* severely compromises virulence and intracellular viability^{6,10–13,51,52,58,62,63}.

Collectively, these studies indicate that cytochrome *bd* can play a role in scavenging exogenous H₂O₂ produced e.g. during infection in a manner similar to periplasmic catalases/peroxidases or SOD, which have been proposed as virulence factors in highly pathogenic bacterial strains among which *E. coli* O157:H7 and several other species^{64–68}.

Two recent studies have suggested that cytochrome *bd* from *E. coli* is endowed with very low guaiacol peroxidase activity⁶⁹ and a significant catalase activity⁷⁰, proposed to explain the protective phenotype of the enzyme *in vivo*.

In the present study, we aimed to investigate the *in vitro* activity of a highly purified preparation of cytochrome *bd* towards hydrogen peroxide. Mass spectrometry showed the presence of a third subunit, CydX. We further show that cytochrome *bd* has quinol peroxidase (QPO) activity and lacks catalase activity. We discuss how the newly discovered QPO activity of cytochrome *bd* can contribute to detoxification of exogenous hydrogen peroxide, therefore potentially contributing to the virulence of pathogenic microorganisms.

Materials and Methods

Materials. Decylubiquinone, Coenzyme Q₀ (UQ-0), 30% hydrogen peroxide (concentration determined using $\epsilon_{240\text{nm}} = 44 \text{ M}^{-1} \text{ cm}^{-171}$), bovine liver catalase and lauroyl sarcosine were purchased from Sigma-Aldrich. 1,4-Dithiothreitol (DDT) was from GERBU. 2-n-Heptyl-4-hydroxyquinoline N-oxide (HQNO) was from Enzo Life Sciences (New York). Lauryl maltoside (LM) was purchased from Affymetrix.

Protein preparation and activity assays. Expression and purification of the wild type cytochrome *bd* was performed using a *cydABX* pACYC177 overexpression vector as described earlier²⁸. For production of the His₆-tagged protein, the vector was modified by addition of six histidine triplets (CACCATCACCACCATCAC) at the 3'-end of *cydA* (C-terminal His₆-tag). Overexpression of the His₆-tagged protein and membrane isolation were done as in²⁸. The protein was purified over a HisTrap Nickel column (GE Healthcare) eluting at ~0.3 M imidazole (0.02–0.5 M imidazole gradient). The protein was further purified using a Superdex 200 gel filtration column (GE Healthcare). The haem *d* content was determined spectrophotometrically from the dithionite-reduced minus as isolated difference spectrum using $\epsilon_{630-650\text{nm}} = 24 \text{ mM}^{-1} \text{ cm}^{-172}$. The protein content was determined with the BCA assay (Uptima, Interchim). The purity of the protein was assessed based on the haem *d*/protein ratio we found (9.26 $\mu\text{mol haem } d/\text{g protein}$) which corresponds to ~97% using a molar weight of 105.5 kDa for His₆-CydABX. Polarographic oxidase activity measurements and lack of catalase activity were performed and confirmed in two groups either using a home-built setup with a Clark-type oxygen electrode⁷³ (Group Simon de

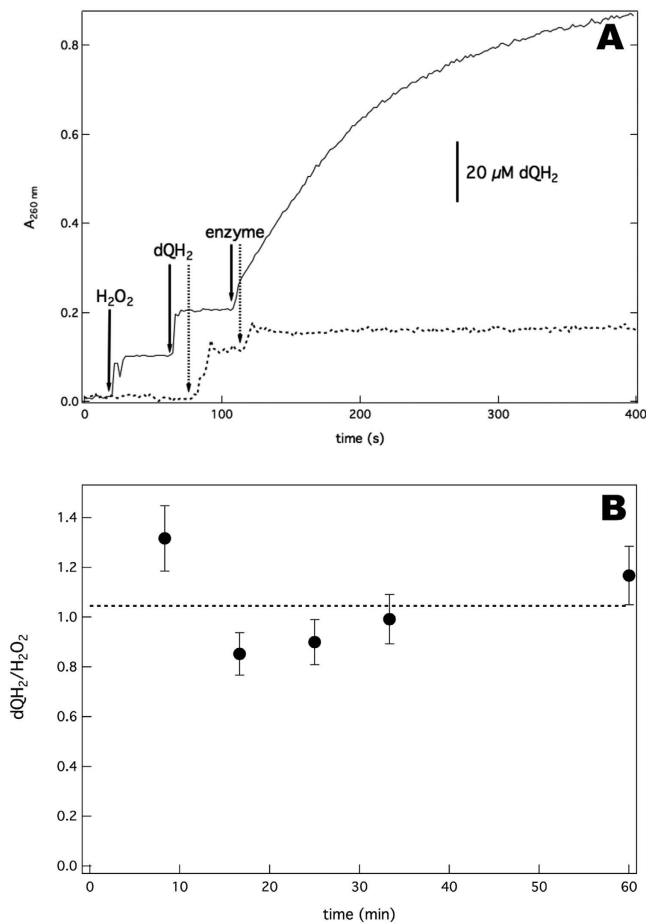


Figure 2. Cytochrome *bd* has quinol peroxidase activity. (A) The QPO reaction catalysed by cytochrome *bd* is monitored as dQH_2 oxidation (260 nm). The dotted trace represents a control experiment where only the enzyme and dQH_2 are added showing a lack of background activity and inferring that the system is anaerobic. Upon addition of H_2O_2 , dQH_2 is oxidized (solid trace). The reaction buffer contained $120\ \mu\text{M dQH}_2$ and $23\ \text{nM}$ cytochrome *bd* with (solid trace) or without (dotted trace) $6\ \text{mM H}_2\text{O}_2$. Solid and dotted arrows indicate the time of the additions corresponding to the solid and dotted traces, respectively. (B) The $\text{dQH}_2/\text{H}_2\text{O}_2$ ratio of the QPO reaction catalysed by cytochrome *bd*. The average $\text{dQH}_2/\text{H}_2\text{O}_2$ ratio was determined at 1.05 ± 0.19 by analyzing the reaction buffer at different time intervals during the reaction. The average ratio is consistent with the peroxidase reaction (Eq. 3). The results are presented as means \pm SD of duplicates ($n = 2$).

Vries) or an Oxygraph + Clark-type oxygen electrode from Hansatech (Group Thorsten Friedrich). Determination of quinol peroxidation rates was conducted inside a Coy anaerobic chamber equipped with an Avantes DH-2000 spectrophotometer. Due to the high 278-nm absorbance at high quinol/quinone concentrations, the reaction progress was monitored at 260 nm rather than 278 nm. The extinction coefficient $\epsilon_{260\text{nm}} = 6.23\ \text{mM}^{-1}\ \text{cm}^{-1}$ was determined from the UV spectrum of decylubiquinol based on $\epsilon_{278\text{nm}} = 12.7\ \text{mM}^{-1}\ \text{cm}^{-1}$. The reactions were performed in the standard buffer: $50\ \text{mM MOPS}$, $100\ \text{mM NaCl}$, $0.1\% \text{ LM}$, pH 7 unless otherwise noted. Aliquots of nitric oxide (NO) were added from a NO-saturated ($2\ \text{mM}$) aqueous solution.

Igor Pro version 6.1 (Wavemetrics) was used for data analysis and creating graphs.

Analysis of the steady-state kinetics. Initial QPO rates were determined for varying H_2O_2 concentrations while keeping the decylubiquinol (dQH_2) concentration constant and *vice versa*. The rates were simulated using the model for a Ping-Pong Bi Bi reaction mechanism according to:

$$\frac{v}{[E]} = \frac{k_{\text{cat}} * [\text{H}_2\text{O}_2] * [\text{dQH}_2]}{K_M^{\text{H}_2\text{O}_2} * [\text{dQH}_2] + K_M^{\text{dQH}_2} * [\text{H}_2\text{O}_2] + [\text{H}_2\text{O}_2] * [\text{dQH}_2]} \quad (2)$$

Herein k_{cat} represents the maximal turnover number (s^{-1}) and $[E]$ the enzyme concentration.

Determination of the reaction stoichiometry. At different time intervals, the QPO reaction ($50\ \mu\text{M H}_2\text{O}_2$, $200\ \mu\text{M dQH}_2$ and $60\ \text{nM}$ cytochrome *bd*) was quenched with $200\ \text{mM HCl}$ and incubated for 2 minutes prior to neutralization with $200\ \text{mM NaOH}$. The concentration of H_2O_2 at each time point was determined using the Amplex Red/Horseradish peroxidase H_2O_2 assay kit (Invitrogen) using $\epsilon_{571\text{nm}} = 58\ \text{mM}^{-1}\ \text{cm}^{-1}$ for resorufin.

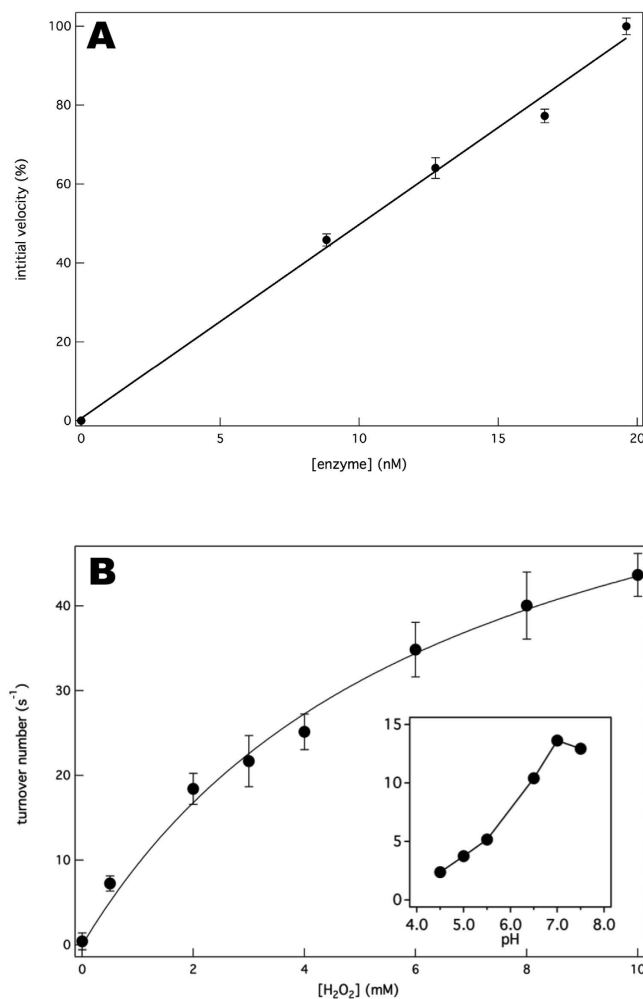


Figure 3. Kinetics of quinol peroxidase activity by cytochrome *bd*. (A) The proportional relation between the initial rate of quinol-peroxide reduction and cytochrome *bd* concentration. The QPO initial rates were measured in standard buffer in the presence of 120 μ M dQH₂ and 1 mM H₂O₂ at room temperature. (B) The QPO activity of cytochrome *bd* as function of the H₂O₂ concentration showing saturation kinetics. Initial rates are expressed as turnover number (mol dQH₂/mol enzyme/s). The data were fitted to the Michaelis-Menten equation (lines). The fitting parameters (apparent V_{\max} and K_M values) were $V_{\max} = 75 \pm 4.5 \text{ s}^{-1}$ and $K_M = 6.6 \pm 1.1 \text{ mM}$. The inset shows the pH-dependence of the QPO reactions at 1 mM H₂O₂. The assays were performed in the presence of 120 μ M dQH₂ and 23 nM cytochrome *bd*. The results are presented as means \pm SD of duplicates ($n = 2$). The inset shows single measurements.

The dQH₂ concentration was determined in the same experiment from the absorbance change at 260 nm as described above.

Determination of catalase activity in membranes. The catalase activity in membranes was determined by following the oxygen production (see above) in standard buffer without detergent at different H₂O₂ concentration. To test whether the catalase activity was membrane-associated, the membranes of *E. coli* overexpressing cytochrome *bd* were washed by first diluting the membrane suspension (1:13) in standard buffer without detergent. The diluted suspension was sonicated (10 min in a Biorupter sonicator from Diagenode at maximum intensity) to disrupt possible membrane vesicles containing cytosolic proteins. The sonicated membrane suspension was centrifuged for 1 h at 300,000 g for membrane recovery. The membrane pellet was resuspended in buffer prior to the polarographic assay. The dilution/sonication procedure was repeated (second wash) using the product from the first step and the polarographic assay was performed again.

Tandem MS analysis and identification of CydX. Purified His-tagged cytochrome *bd* was loaded on a Native-PAGE, the protein band of interest was excised from the gel and subjected to in gel proteolytic digestion using either trypsin, chymotrypsin or GluC (enzyme: protein ratios \sim 1:15–1:20 (w/w) in 25 mM ammonium bicarbonate, pH 8.1) overnight at 37 °C. Prior to digestion, cysteines were reduced with dithiothreitol (DTT) in ammonium bicarbonate for 30 min, followed by alkylation with iodoacetamide in ammonium bicarbonate in the dark for 45 min. In-gel digests were separated and analyzed on EASY-nLC 1000 system directly coupled to a

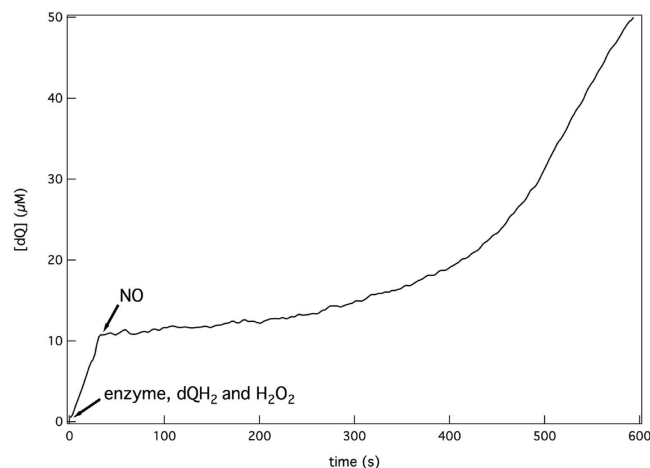


Figure 4. Inhibition of quinol peroxidase activity by nitric oxide. Reversible inhibition of the QPO reaction by NO was monitored spectrophotometrically. After addition of $6\ \mu\text{M}$ NO, the reaction is inhibited promptly but resumes due to disappearance of NO. The QPO reaction was started by addition of $200\ \mu\text{M}$ dQH₂ and $10\ \text{mM}$ H₂O₂ to $9\ \text{nM}$ of cytochrome *bd* at room temperature.

Q Exactive Plus mass spectrometer (Thermo, Bremen, Germany). Peptides were separated on a reversed-phase column (Acclaim PepMap, $50\ \mu\text{m} \times 150\ \text{mm}$, $2\ \mu\text{m}$, $100\ \text{\AA}$, Thermo, Bremen, Germany). The gradient was from 100% Solvent A (0.1% formic acid in water) to 60% solvent B (acetonitrile) in 25 min. at a flow rate of $500\ \text{nl}/\text{min}$. The column effluent was directly electrosprayed in the ESI source of the mass spectrometer using a nano-ESI emitter (Nano-bore emitter, Thermo, Bremen, Germany). MS data was acquired in the positive ion mode using a data-dependent top10 analysis method. Full scan spectra were acquired in the m/z range 400–1200 at a resolution of 70,000, a target value of $3e6$ and a maximum injection time of 100 msec. HCD fragmentation events were dynamically triggered at an underfill ratio of 5%. Isolation of precursor ions was done with a window of 2.5 amu, a target value of $2e5$ and maximum injection time of 50 msec. Normalized collision energy of 27 eV was used and fragment ions were acquired at a resolution of 17,500 with m/z 100 as first mass. The raw data was processed with Proteome Discoverer 1.4 (Thermo, Bremen, Germany) and spectra were matched against the Uniprot protein database using mascot. Search parameters used were; 5 ppm for precursor mass, 0.02 Da for fragment ions, taxonomy restrain *E. coli*, carbamidomethylcysteine as fixed modification and oxidized methionine as variable modification and no cleavage enzyme was specified. CydX from *E. coli* consists of 37 amino acid residues (1-MWYFAWILGTLLACSFVITALALEHVESGKAGQEDI-37).

Analytical chromatography. To verify the monodispersity of the pure cytochrome *bd*, $500\ \mu\text{g}$ of the enzyme was loaded onto a gel filtration column (Superose 6 $10/300\ \text{gl}$, GE Healthcare) equilibrated with the standard buffer (VE2001 GPC solvent/sample module, Viscotek). The UV absorbance at 280 nm (UV Detector 2600, Viscotek) as well as the refractive index and the right angle light scattering were monitored during the run (TDA 305 triple detector array, Viscotek).

Results

The cytochrome *bd* preparation is highly pure and contains the CydX subunit. Using decylubiquinol (dQH₂) as electron donor, the purified cytochrome *bd* displayed a turnover number of $185 \pm 15\ \text{dQH}_2\ \text{s}^{-1}$ consistent with the value for the wild-type enzyme⁷² indicating that the His-tag did not interfere with the activity of the enzyme. Cytochrome *bd* has long been considered a hetero-dimer throughout literature^{1–3,20}. However, recent mutational studies in *E. coli*, *Brucella abortus* and *Shewanella oneidensis* suggested that the small protein, CydX (37, 64 and 38 amino acids in *E. coli*, *B. abortus* and *S. oneidensis*, resp.) is important for assembly, stability and activity of cytochrome *bd* *in vivo* and *in vitro*^{63,74–76}. The presence of CydX has also been confirmed in purified cytochrome *bd*⁷⁵. To confirm the presence of CydX in our preparation we performed a mass-spectrometric analysis. Using trypsin, chymotrypsin and Glu-C to cleave the protein we detected the peptides 23-ALEHVESGKAGQEDI-37, 29-SGKAGQEDI-37 and 23-ALEHVESGKAGQEDI-37, respectively, unequivocally confirming the presence of CydX in our preparation. To verify the monodispersity of the purified cytochrome *bd*, the enzyme was subjected to analytical chromatography (Fig. 1). The UV absorption showed a single peak, corresponding to the mass of the cytochrome *bd* tetramer including the LM micelle (approx. 480 kDa). Refractive index and right angle light scattering exhibited a second peak (approx. 70 kDa) corresponding to the average size of an empty LM micelle. Based on the haem *d*/protein ratio (see Materials and Methods) the protein purity was approximated as ~97%. These results show that the isolated cytochrome *bd* is pure, active and complete.

Cytochrome *bd* is a quinol peroxidase. We tested whether cytochrome *bd* could function as a peroxidase with its natural oxidase substrate, ubiquinol. Reduced decylubiquinol was used as replacement for the natural

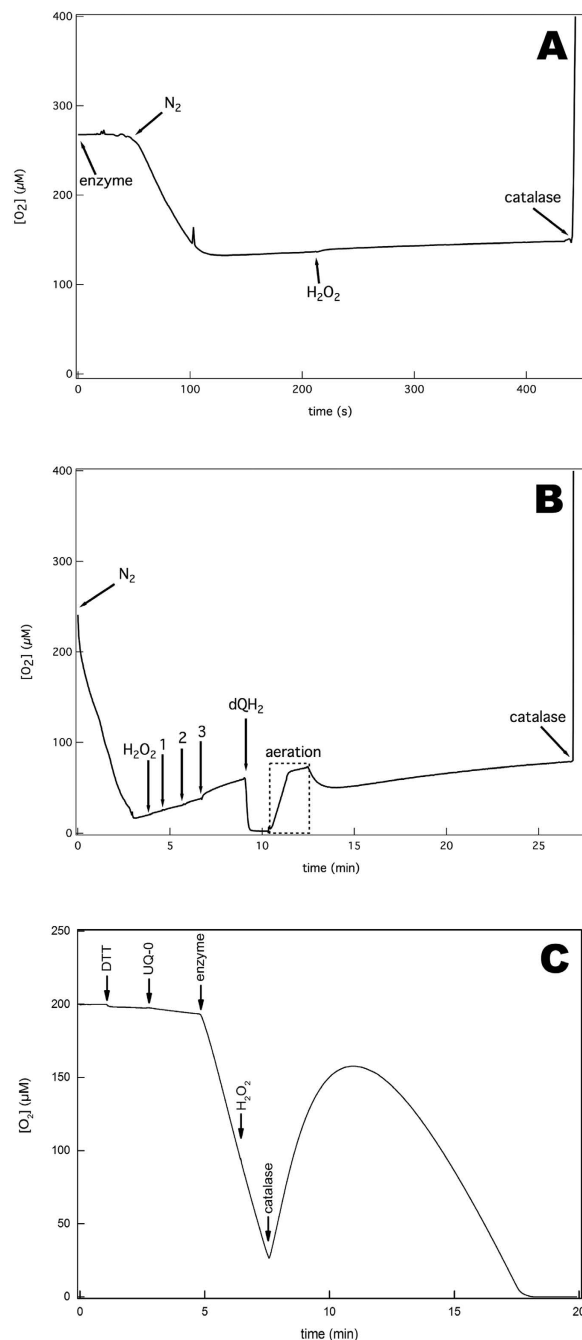


Figure 5. Lack of catalase activity of purified cytochrome *bd* in non- and mid-turnover conditions.

(A) Oxygen measurement in the presence of cytochrome *bd* and H₂O₂ shows that the enzyme does not have catalase activity. The enzyme (125 nM) in standard buffer was first purged with nitrogen gas (N₂) to lower the oxygen concentration to ~130 μM. The addition of 1 mM H₂O₂ did not show any generation of oxygen indicating the lack of catalase activity. As a positive control, 1 μM of catalase was added resulting in a rapid increase in oxygen concentration. Due to oxygen leakage into the measuring chamber, a slow background increase in oxygen concentration is observed. (B) Test for catalase activity by cytochrome *bd* using buffer and detergent reported in⁷⁰. Lack of catalase activity of cytochrome *bd* determined polarographically. The buffer was 50 mM KPi, 0.1 mM EDTA, 0.05% LS, pH 7.0 the same as in⁷⁰. The buffer was purged with nitrogen gas (N₂) to lower the oxygen concentration prior to addition of 1 mM H₂O₂. Then, cytochrome *bd* was added successively indicated by numbered arrows: 1, 0.075 μM; 2, 0.225 μM and 3, 1 μM (accumulative concentrations). No catalase activity was detected after any of these additions. When 200 μM dQH₂ was added a rapid decrease in oxygen concentration is observed due to the oxidase activity of cytochrome *bd*. (C) Polarographic test for catalase activity during turnover as previously reported in⁷⁰. Oxidase turnover was started, by consecutively adding 10 mM DTT, 50 μM UQ-0 and 100 nM enzyme to the standard buffer. During turnover 1 mM of H₂O₂ was added to the reaction and a decrease in oxidase activity of 9 ± 2% could be observed. Oxygen formation was only observed after adding 20 nM catalase.

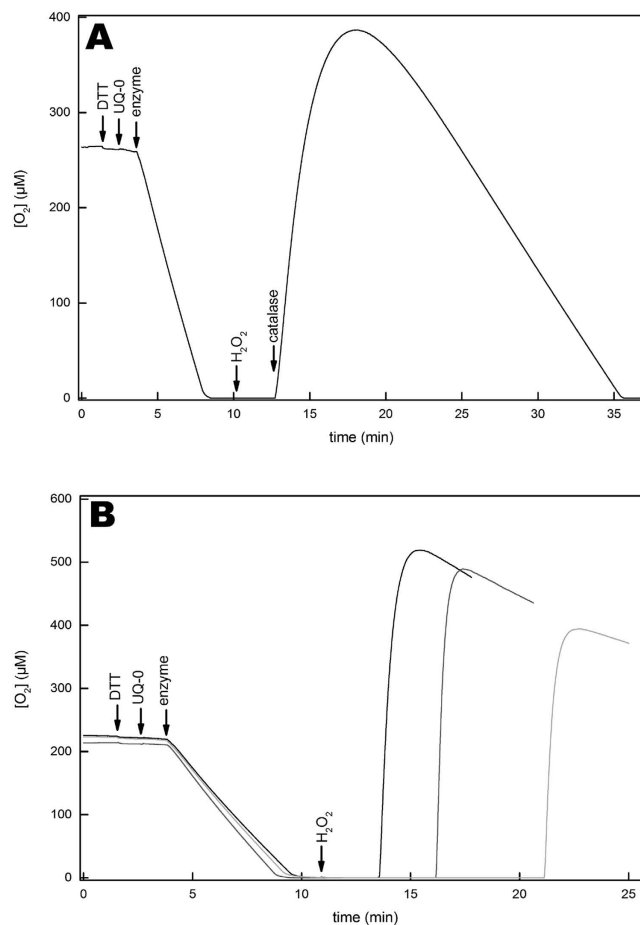


Figure 6. Lack of catalase activity of purified cytochrome *bd* in post-turnover conditions. Polarographic test for catalase activity after achieving anoxia through cytochrome *bd* oxidase turnover as in⁷⁰. **(A)** Oxidase turnover was started, by consecutively adding 10 mM DTT, 50 μM UQ-0 and 100 nM enzyme to the standard buffer. 90 seconds after reaching anoxia, 1 mM of H₂O₂ was added to the reaction and no increase in oxygen could be observed. 150 seconds after peroxide addition, 20 nM catalase were added and formation of oxygen was observed. **(B)** Identical reaction parameters as in **(A)** were used. The reaction mixture was incubated for 2.5 (black), 5 (gray) and 10 minutes (light gray) after addition of 1 mM H₂O₂. After incubation, 100 nM of catalase were added and formation of different quantities of oxygen was observed.

ubiquinol-8 in *E. coli*⁷² and its oxidation was followed spectrophotometrically in the presence of H₂O₂ (Eq. 3). Experiments were carried-out strictly anaerobically to prevent interference between the oxidase and peroxidase reactions. Cytochrome *bd* was found to catalyse the oxidation of dQH₂ in the presence of H₂O₂ (Fig. 2A). To confirm that the oxidation of dQH₂ is due to dQH₂:H₂O₂ oxidoreduction, i.e. QPO activity, we measured the amounts of both H₂O₂ and dQH₂ consumed in time in order to determine the reaction stoichiometry. Figure 2B shows the calculated ratios of dQH₂/H₂O₂, which average to 1.05 ± 0.19. This is consistent with the 1:1 stoichiometry predicted for a genuine QPO reaction (Eq. 3).



To investigate the steady-state kinetics of the QPO reaction, the initial peroxidation rates were measured at different enzyme, H₂O₂ and dQH₂ concentrations. The plot of initial rate versus the amount of enzyme shows a linear relationship (Fig. 3A). The K_M values for H₂O₂ and dQH₂ were determined at 6.6 ± 1.1 mM and 72 ± 20 μM, respectively, with the latter being similar to the K_M (dQH₂) of 85 ± 5 μM⁷² of the oxidase reaction (Fig. 3B). The maximal QPO *k*_{cat} calculated according to Eq. 2 was 101 ± 10 H₂O₂ s⁻¹ yielding a specificity constant *k*_{cat}/K_M (H₂O₂) = 1.5 × 10⁴ M⁻¹ s⁻¹. The QPO pH-dependence profile (inset Fig. 3B) is similar to that of the oxidase reaction⁷⁷, with the highest activity at around pH 7. However, the oxidase reaction is completely inhibited at pH values lower than 5.5⁷⁷ whereas at this pH the QPO reaction retains ~1/3 of its maximal value at pH 7.0.

The QPO reaction is inhibited by oxidase inhibitors. NO which mainly binds haem *d*²⁷, is a reversible inhibitor of the oxidase reaction⁷⁸. Interestingly, our data show that also the QPO reaction is inhibited by NO as well (Fig. 4). Upon addition of 6 μM NO, dQH₂ oxidation was drastically decreased. The inhibition was reversible as the activity slowly restored (Fig. 4), likely due to slow reaction between NO and dQH₂ which was observed

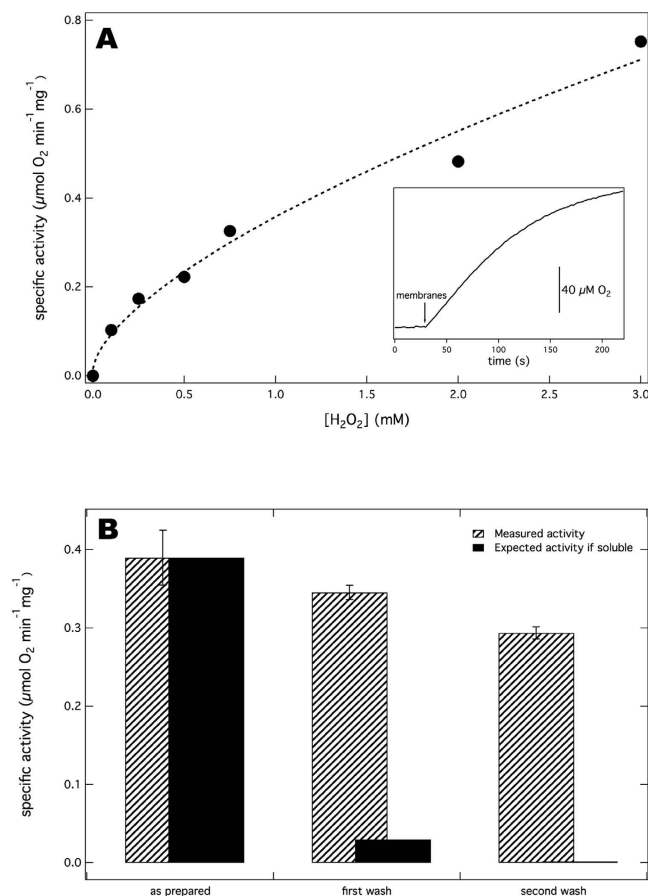


Figure 7. Catalase activity in an *E. coli* membrane fraction. (A) The dependence of the catalase activity of isolated *E. coli* membranes on H₂O₂ concentration. Membranes were added to H₂O₂ containing standard buffer. The dashed line is a non-hyperbolic power law fit: Specific activity = $y_0 + A * [H_2O_2]^n$, where $y_0 = 0.015$, $A = 0.34$ and $n = 0.65$. The inset is a representative activity trace that shows oxygen formation in the presence of 0.25 mM H₂O₂. (B) The catalase activity is membrane-associated. A weak catalase activity measured at 1 mM H₂O₂ was observed in the membranes of *E. coli*. The bulk of the catalase activity (striped bars) was resistant to washing/sonication cycles (See Materials and Methods) indicating that the activity is membrane-associated. A theoretical activity profile (solid bars) is shown representing the expected remaining catalase activity for a soluble entity (7.7% and 0.60% remaining activity after the first and second washing steps, respectively). The results are presented as means \pm SD of duplicates ($n = 2$).

in a separate experiment (22 nM s⁻¹ NO at 100 μM NO and 100 μM dQH₂, data not shown). We did not detect a reaction between NO and H₂O₂ or any quinol:NO reductase activity, in agreement with others⁷⁸. We also found that titration of the QPO and oxidase activities with HQNO shows that 50% inhibition is obtained at ~10–15 μM for both reactions.

Cytochrome *bd* does not show catalase activity. Catalases produce oxygen and water from hydrogen peroxide (Eq. 4) allowing the detection of their activity polarographically using a Clark-type oxygen sensor. Recently it was reported that cytochrome *bd* from *E. coli* had catalase activity⁷⁰. We tested our pure cytochrome *bd* preparation polarographically in standard buffer (Fig. 5A) and in the buffer (50 mM KP₁ + 0.1 mM EDTA + 0.05% N-lauroylsarcosine, pH 7.0) used in ref. 70 (Fig. 5B). Even at enzyme concentrations as high as 1 μM cytochrome *bd* (Fig. 5B), catalase activity was absent. In Fig. 5C we show our attempt to reproduce the mid-turnover catalase activity measurement shown in ref. 70. Albeit we noticed a decrease of oxidase activity of $9 \pm 2\%$ upon addition of 1 mM H₂O₂ to the assay during turnover (Fig. 5C), we were not able to detect catalase activity under neither of these assay conditions. The lack of post-turnover catalase activity shown in Fig. 3 in ref. 70 was confirmed using similar reaction parameters (Fig. 6A). Interestingly, we observed that the quantity of released oxygen upon catalase addition is dependent of the incubation time of the enzyme with H₂O₂ (Fig. 6B). This supports the conclusion that H₂O₂ is consumed during the incubation process, but no oxygen is released, i.e. due to the QPO activity (Eq. 3).



We hypothesized that the catalase activity detected by the authors in ref. 70 might be due to impurities in their enzyme preparation. Therefore, isolated membranes from *E. coli* that overexpress cytochrome *bd* were assayed

for catalase activity. Interestingly, the membranes did show a weak catalase activity (Fig. 7). It is notable that the relation between activity and H_2O_2 concentration (Fig. 7A) is very similar to that presented in the inset of Fig. 1 in ref. 70. The catalase activity profile is biphasic and non-hyperbolic, showing quite a sharp increase below ~ 0.2 mM H_2O_2 and levelling off at higher H_2O_2 concentrations unlike canonical catalases that show a linear relation at millimolar H_2O_2 concentrations^{79–81}. These data suggest that the catalase activity reported in ref. 70 is due to an impurity in the cytochrome *bd* preparation, although we cannot rule out the possibility that the catalase activity may be dependent on the experimental conditions chosen for protein expression and purification.

To determine if the catalase activity we found in the membrane suspension is membrane-associated and not a cytosolic entity, the activity was measured after washing and sonicating the membranes in buffer containing no detergent (see Materials and Methods). The weak catalase activity decreased slightly after each washing step (Fig. 7B, striped bars), which is prescribed to inactivation and loss of material during the washing procedure. The results show that this catalase activity is resistant to washing suggesting it is membrane-associated. The catalases (KatG and KatE) in *E. coli* are soluble proteins and to our knowledge, no membrane-bound catalases have been reported in *E. coli*. Our results show the presence of an unknown membrane-associated catalase activity in *E. coli*. This hitherto unidentified catalase activity was not further investigated in this study.

Discussion

The purpose of this study was to investigate the *in vitro* activity of cytochrome *bd* with hydrogen peroxide to highlight its potential anti-ROS activity *in vivo*. We have demonstrated here that cytochrome *bd* from *E. coli* is a bifunctional enzyme equipped with quinol-linked oxygen and H_2O_2 reduction activities. In addition, we have shown that the QPO reaction is inhibited by HQNO and NO similar to the oxidase reaction, which suggests a similar involvement of the haem centres and the quinol-binding site in both the oxidase and QPO reactions in respect to electron transfer and catalysis. Under the conditions employed in this study, the data showed that cytochrome *bd* does not function as a catalase. However, we did detect a membrane-associated catalase activity in isolated *E. coli* membranes not documented before that showed an unusual relation between activity and H_2O_2 concentration.

Quinol peroxidation is quite rare in prokaryotes. Besides cytochrome *bd*, another QPO was found in the human pathogen *Aggregatibacter actinomycetemcomitans*. This enzyme is a tri-haem *c* membrane-bound protein with $\sim 43\%$ sequence identity with bacterial cytochrome *c* peroxidases but less than 13% with cytochrome *bd*^{82,83}. Inhibition of AcQPO correlated to decreased pathogenicity of *A. actinomycetemcomitans*⁸³, a phenotype typical for cytochrome *bd* mutants (see below). *E. coli* contains a homologue of AcQPO (YhjA⁸²) predicted to be a cytochrome *c* peroxidase⁴³. YhjA was also tested for QPO activity and was found negative⁸². To our knowledge, cytochrome *bd* is the first quinol peroxidase characterized in *E. coli*.

The QPO activity of cytochrome *bd* demonstrated could provide direct biochemical underpinning for understanding some phenotypes displayed by organisms with non-functional cytochrome *bd*. For example *E. coli* with disrupted cytochrome *bd* accumulated temperature-sensitive growth defects, which could be reverted by exogenous addition of reducing agents as well as SOD and catalase suggesting that increased ROS concentrations (induced at higher temperatures) can be counteracted by the peroxidative cytochrome *bd* activity⁸⁴. The localization of cytochrome *bd* in the membrane, suggests that the enzyme can reduce exogenous H_2O_2 and is therefore functionally differentiated from Ahp, KatG and KatE that scavenge intracellular H_2O_2 ^{32,85–88}.

As described in the Introduction^{6,10–13,51,52,58,62,63,89}, many examples indicate that pathogenic bacteria that lack cytochrome *bd* activity display compromised virulence and viability. A striking example is provided by the *in vivo* anti-ROS activity of cytochrome *bd* in the gram-negative pathogen *B. abortus*⁶. *B. abortus* devoid of a functional cytochrome *bd* had severely compromised survival in murine spleens, but in *trans* over-expression of SOD, catalase or cytochrome *bd* complemented this phenotype showing that H_2O_2 accumulation is the main phenotype induced by lack of cytochrome *bd* activity⁶. Consistent with this finding, *Staphylococcus aureus* increases cytochrome *bd* expression 8–9 fold upon addition of 10 mM H_2O_2 ⁹⁰ and *M. tuberculosis* with over-expressed cytochrome *bd* showed increased resistance to H_2O_2 ⁹¹, whereas a cytochrome *bd* knockout in this strain resulted in decreased survival in the mammalian host¹⁰. The predicted localization of the cytochrome *bd* active site at the periplasmic side of the cytoplasmic membrane may testify to its protective function mainly against environmentally produced H_2O_2 and against H_2O_2 produced in the phagocyte oxidative burst experienced by pathogenic bacteria residing in human macrophages. The finding that the oxidase reaction is completely inhibited at pH values lower than 5.5⁷⁷ but the QPO reaction of cytochrome *bd* is not, may be relevant to its role in combatting the phagocyte oxidative burst in view of the low pH in the phagocyte⁹². It would be important to test cytochrome *bd* from pathogenic bacterial strains for QPO activity, and to evaluate the contribution of the QPO for survival in the host.

In summary, our finding that cytochrome *bd* exhibits QPO activity demonstrates that this respiratory complex can serve as a detoxifying enzyme.

In addition to indirectly decreasing the rate of intracellular ROS production via its oxidase reaction, cytochrome *bd* can also actively metabolize and detoxify hydrogen peroxide. As such, the very catalytic properties of cytochrome *bd* may explain how the enzyme can act as general virulence factor, which operates in concert with other virulence factors enhancing pathogenicity.

References

1. Borisov, V. B., Gennis, R. B., Hemp, J. & Verkhovskiy, M. I. The cytochrome *bd* respiratory oxygen reductases. *Biochim. Biophys. Acta* **1807**, 1398–1413, doi: 10.1016/j.bbabi.2011.06.016 (2011).
2. Junemann, S. Cytochrome *bd* terminal oxidase. *Biochim. Biophys. Acta* **1321**, 107–127 (1997).
3. Miller, M. J. & Gennis, R. B. The purification and characterization of the cytochrome *d* terminal oxidase complex of the *Escherichia coli* aerobic respiratory chain. *J. Biol. Chem.* **258**, 9159–9165 (1983).

4. Kita, K., Konishi, K. & Anraku, Y. Terminal oxidases of *Escherichia coli* aerobic respiratory chain. II. Purification and properties of cytochrome b558-d complex from cells grown with limited oxygen and evidence of branched electron-carrying systems. *J. Biol. Chem.* **259**, 3375–3381 (1984).
5. Baughn, A. D. & Malamy, M. H. The strict anaerobe *Bacteroides fragilis* grows in and benefits from nanomolar concentrations of oxygen. *Nature* **427**, 441–444, doi: 10.1038/nature02285 (2004).
6. Endley, S., McMurray, D. & Ficht, T. A. Interruption of the *cydB* locus in *Brucella abortus* attenuates intracellular survival and virulence in the mouse model of infection. *J. Bacteriol.* **183**, 2454–2462, doi: 10.1128/JB.183.8.2454-2462.2001 (2001).
7. Juty, N. S., Moshiri, F., Merrick, M., Anthony, C. & Hill, S. The *Klebsiella pneumoniae* cytochrome *bd*⁺ terminal oxidase complex and its role in microaerobic nitrogen fixation. *Microbiology* **143** (Pt 8), 2673–2683 (1997).
8. Larsen, M. H., Kallipolitis, B. H., Christiansen, J. K., Olsen, J. E. & Ingmer, H. The response regulator ResD modulates virulence gene expression in response to carbohydrates in *Listeria monocytogenes*. *Mol. Microbiol.* **61**, 1622–1635, doi: 10.1111/j.1365-2958.2006.05328.x (2006).
9. Loisel-Meyer, S., Jimenez de Bagues, M. P., Kohler, S., Liautard, J. P. & Jubier-Maurin, V. Differential use of the two high-oxygen-affinity terminal oxidases of *Brucella suis* for *in vitro* and intramacrophagic multiplication. *Infect. Immun.* **73**, 7768–7771, doi: 10.1128/IAI.73.11.7768-7771.2005 (2005).
10. Shi, L. *et al.* Changes in energy metabolism of *Mycobacterium tuberculosis* in mouse lung and under *in vitro* conditions affecting aerobic respiration. *Proc. Natl. Acad. Sci. USA* **102**, 15629–15634, doi: 10.1073/pnas.0507850102 (2005).
11. Turner, A. K. *et al.* Contribution of proton-translocating proteins to the virulence of *Salmonella enterica* serovars Typhimurium, Gallinarum, and Dublin in chickens and mice. *Infect. Immun.* **71**, 3392–3401 (2003).
12. Way, S. S., Sallustio, S., Magliozzo, R. S. & Goldberg, M. B. Impact of either elevated or decreased levels of cytochrome *bd* expression on *Shigella flexneri* virulence. *J. Bacteriol.* **181**, 1229–1237 (1999).
13. Yamamoto, Y. *et al.* Respiration metabolism of Group B *Streptococcus* is activated by environmental haem and quinone and contributes to virulence. *Mol. Microbiol.* **56**, 525–534, doi: 10.1111/j.1365-2958.2005.04555.x (2005).
14. Zhang-Barber, L. *et al.* Influence of genes encoding proton-translocating enzymes on suppression of *Salmonella typhimurium* growth and colonization. *J. Bacteriol.* **179**, 7186–7190 (1997).
15. Jasaitis, A. *et al.* Electrogenic reactions of cytochrome *bd*. *Biochemistry* **39**, 13800–13809 (2000).
16. Puustinen, A., Finel, M., Haltia, T., Gennis, R. B. & Wikstrom, M. Properties of the two terminal oxidases of *Escherichia coli*. *Biochemistry* **30**, 3936–3942 (1991).
17. Bertsova, Y. V., Bogachev, A. V. & Skulachev, V. P. Generation of protonic potential by the *bd*-type quinol oxidase of *Azotobacter vinelandii*. *FEBS Lett.* **414**, 369–372 (1997).
18. Kolonay, J. E., Jr. & Maier, R. J. Formation of pH and potential gradients by the reconstituted *Azotobacter vinelandii* cytochrome *bd* respiratory protection oxidase. *J. Bacteriol.* **179**, 3813–3817 (1997).
19. Miller, M. J. & Gennis, R. B. The cytochrome *d* complex is a coupling site in the aerobic respiratory chain of *Escherichia coli*. *J. Biol. Chem.* **260**, 14003–14008 (1985).
20. Al-Attar, S. & de Vries, S. Energy transduction by respiratory metallo-enzymes: From molecular mechanism to cell physiology. *Coord. Chem. Rev.* **257**, 64–80, doi: 10.1016/J.Ccr.2012.05.022 (2013).
21. Safarian, S. *et al.* Structure of a *bd* oxidase indicates similar mechanisms for membrane-integrated oxygen reductases. *Science* **352**, 583–586 (2016).
22. Arutyunyan, A. M. *et al.* Strong excitonic interactions in the oxygen-reducing site of *bd*-type oxidase: the Fe-to-Fe distance between hemes *d* and *b595* is 10 Å. *Biochemistry* **47**, 1752–1759, doi: 10.1021/bi701884g (2008).
23. Hill, J. J., Alben, J. O. & Gennis, R. B. Spectroscopic evidence for a heme-heme binuclear center in the cytochrome *bd* ubiquinol oxidase from *Escherichia coli*. *Proc. Natl. Acad. Sci. USA* **90**, 5863–5867 (1993).
24. Rappaport, F., Zhang, J., Vos, M. H., Gennis, R. B. & Borisov, V. B. Heme-heme and heme-ligand interactions in the di-heme oxygen-reducing site of cytochrome *bd* from *Escherichia coli* revealed by nanosecond absorption spectroscopy. *Biochim. Biophys. Acta* **1797**, 1657–1664, doi: 10.1016/j.bbabi.2010.05.010 (2010).
25. Vos, M. H., Borisov, V. B., Liebl, U., Martin, J. L. & Konstantinov, A. A. Femtosecond resolution of ligand-heme interactions in the high-affinity quinol oxidase *bd*: A di-heme active site? *Proc. Natl. Acad. Sci. USA* **97**, 1554–1559, doi: 10.1073/pnas.030528197 (2000).
26. Belevich, I. *et al.* Time-resolved electrometric and optical studies on cytochrome *bd* suggest a mechanism of electron-proton coupling in the di-heme active site. *Proc. Natl. Acad. Sci. USA* **102**, 3657–3662, doi: 10.1073/pnas.0405683102 (2005).
27. Borisov, V., Arutyunyan, A. M., Osborne, J. P., Gennis, R. B. & Konstantinov, A. A. Magnetic circular dichroism used to examine the interaction of *Escherichia coli* cytochrome *bd* with ligands. *Biochemistry* **38**, 740–750, doi: 10.1021/bi981908t (1999).
28. Paulus, A., Rossius, S. G., Dijk, M. & de Vries, S. Oxoferryl-porphyrin radical catalytic intermediate in cytochrome *bd* oxidases protects cells from formation of reactive oxygen species. *J. Biol. Chem.* **287**, 8830–8838, doi: 10.1074/jbc.M111.333542 (2012).
29. Massey, V. *et al.* The production of superoxide anion radicals in the reaction of reduced flavins and flavoproteins with molecular oxygen. *Biochem. Biophys. Res. Commun.* **36**, 891–897 (1969).
30. Messner, K. R. & Imlay, J. A. The identification of primary sites of superoxide and hydrogen peroxide formation in the aerobic respiratory chain and sulfite reductase complex of *Escherichia coli*. *J. Biol. Chem.* **274**, 10119–10128 (1999).
31. Messner, K. R. & Imlay, J. A. Mechanism of superoxide and hydrogen peroxide formation by fumarate reductase, succinate dehydrogenase, and aspartate oxidase. *J. Biol. Chem.* **277**, 42563–42571, doi: 10.1074/jbc.M204958200 (2002).
32. Seaver, L. C. & Imlay, J. A. Alkyl hydroperoxide reductase is the primary scavenger of endogenous hydrogen peroxide in *Escherichia coli*. *J. Bacteriol.* **183**, 7173–7181, doi: 10.1128/JB.183.24.7173-7181.2001 (2001).
33. Korshunov, S. & Imlay, J. A. Two sources of endogenous hydrogen peroxide in *Escherichia coli*. *Mol. Microbiol.* **75**, 1389–1401, doi: 10.1111/j.1365-2958.2010.07059.x (2010).
34. Kussmaul, L. & Hirst, J. The mechanism of superoxide production by NADH:ubiquinone oxidoreductase (complex I) from bovine heart mitochondria. *Proc. Natl. Acad. Sci. USA* **103**, 7607–7612, doi: 10.1073/pnas.0510977103 (2006).
35. Wardman, P. & Candeias, L. P. Fenton chemistry: an introduction. *Radiat. Res.* **145**, 523–531 (1996).
36. Imlay, J. A. The molecular mechanisms and physiological consequences of oxidative stress: lessons from a model bacterium. *Nat. Rev. Microbiol.* **11**, 443–454, doi: 10.1038/nrmicro3032 (2013).
37. Jang, S. & Imlay, J. A. Hydrogen peroxide inactivates the *Escherichia coli* *Isc* iron-sulphur assembly system, and *OxyR* induces the *Suf* system to compensate. *Mol. Microbiol.* **78**, 1448–1467, doi: 10.1111/j.1365-2958.2010.07418.x (2010).
38. Py, B. & Barras, F. Building Fe-S proteins: bacterial strategies. *Nat. Rev. Microbiol.* **8**, 436–446, doi: 10.1038/nrmicro2356 (2010).
39. Craig, M. & Schlauch, J. M. Phagocytic superoxide specifically damages an extracytoplasmic target to inhibit or kill *Salmonella*. *PLoS One* **4**, e4975, doi: 10.1371/journal.pone.0004975 (2009).
40. Schlauch, J. M. How does the oxidative burst of macrophages kill bacteria? Still an open question. *Mol. Microbiol.* **80**, 580–583, doi: 10.1111/j.1365-2958.2011.07612.x (2011).
41. Miller, R. A. & Britigan, B. E. Role of oxidants in microbial pathophysiology. *Clinical microbiology reviews* **10**, 1–18 (1997).
42. Imlay, J. A. Cellular defenses against superoxide and hydrogen peroxide. *Annu. Rev. Biochem.* **77**, 755–776, doi: 10.1146/annurev.biochem.77.061606.161055 (2008).
43. Partridge, J. D., Poole, R. K. & Green, J. The *Escherichia coli* *yjhA* gene, encoding a predicted cytochrome *c* peroxidase, is regulated by FNR and *OxyR*. *Microbiology* **153**, 1499–1507, doi: 10.1099/mic.0.2006/004838-0 (2007).

44. Storz, G. & Imlay, J. A. Oxidative stress. *Current opinion in microbiology* **2**, 188–194 (1999).
45. Arenas, F. A. *et al.* The *Escherichia coli* *btuE* gene, encodes a glutathione peroxidase that is induced under oxidative stress conditions. *Biochim. Biophys. Res. Commun.* **398**, 690–694, doi: 10.1016/j.bbrc.2010.07.002 (2010).
46. Arenas, F. A. *et al.* The *Escherichia coli* *BtuE* protein functions as a resistance determinant against reactive oxygen species. *PLoS One* **6**, e15979, doi: 10.1371/journal.pone.0015979 (2011).
47. Cha, M. K., Kim, W. C., Lim, C. J., Kim, K. & Kim, I. H. *Escherichia coli* periplasmic thiol peroxidase acts as lipid hydroperoxide peroxidase and the principal antioxidative function during anaerobic growth. *J. Biol. Chem.* **279**, 8769–8778, doi: 10.1074/jbc.M312388200 (2004).
48. Jeong, W., Cha, M. K. & Kim, I. H. Thioredoxin-dependent hydroperoxide peroxidase activity of bacterioferritin comigratory protein (BCP) as a new member of the thiol-specific antioxidant protein (TSA)/Alkyl hydroperoxide peroxidase C (AhpC) family. *J. Biol. Chem.* **275**, 2924–2930 (2000).
49. Kelly, M. J., Poole, R. K., Yates, M. G. & Kennedy, C. Cloning and mutagenesis of genes encoding the cytochrome *bd* terminal oxidase complex in *Azotobacter vinelandii*: mutants deficient in the cytochrome *d* complex are unable to fix nitrogen in air. *J. Bacteriol.* **172**, 6010–6019 (1990).
50. Leung, D. *et al.* Mutagenesis of a gene encoding a cytochrome *o*-like terminal oxidase of *Azotobacter vinelandii*: a cytochrome *o* mutant is aero-tolerant during nitrogen fixation. *FEMS Microbiol. Lett.* **119**, 351–357 (1994).
51. Giuffrè, A., Borisov, V. B., Arese, M., Sarti, P. & Forte, E. Cytochrome *bd* oxidase and bacterial tolerance to oxidative and nitrosative stress. *Biochim. Biophys. Acta* **1837**, 1178–1187, doi: 10.1016/j.bbabi.2014.01.016 (2014).
52. Mason, M. G. *et al.* Cytochrome *bd* confers nitric oxide resistance to *Escherichia coli*. *Nat. Chem. Biol.* **5**, 94–96, doi: 10.1038/nchembio.135 (2009).
53. Poole, R. K. & Cook, G. M. Redundancy of aerobic respiratory chains in bacteria? Routes, reasons and regulation. *Adv. Microb. Physiol.* **43**, 165–224 (2000).
54. Lindqvist, A., Membrillo-Hernandez, J., Poole, R. K. & Cook, G. M. Roles of respiratory oxidases in protecting *Escherichia coli* K12 from oxidative stress. *Antonie Van Leeuwenhoek* **78**, 23–31 (2000).
55. Hill, S., Viollet, S., Smith, A. T. & Anthony, C. Roles for enteric *d*-type cytochrome oxidase in N₂ fixation and microaerobiosis. *J. Bacteriol.* **172**, 2071–2078 (1990).
56. Edwards, S. E. *et al.* Mutation of cytochrome *bd* quinol oxidase results in reduced stationary phase survival, iron deprivation, metal toxicity and oxidative stress in *Azotobacter vinelandii*. *FEMS Microbiol. Lett.* **185**, 71–77 (2000).
57. Wall, D. *et al.* *arc*-dependent thermal regulation and extragenic suppression of the *Escherichia coli* cytochrome *d* operon. *J. Bacteriol.* **174**, 6554–6562 (1992).
58. Lu, P. *et al.* The cytochrome *bd*-type quinol oxidase is important for survival of *Mycobacterium smegmatis* under peroxide and antibiotic-induced stress. *Scientific reports* **5**, 10333, doi: 10.1038/srep10333 (2015).
59. Dwyer, D. J. *et al.* Antibiotics induce redox-related physiological alterations as part of their lethality. *Proc. Natl. Acad. Sci. USA* **111**, E2100–2109, doi: 10.1073/pnas.1401876111 (2014).
60. Hards, K. *et al.* Bactericidal mode of action of bedaquiline. *J. Antimicrob. Chemother.* **70**, 2028–2037, doi: 10.1093/jac/dkv054 (2015).
61. Berney, M., Hartman, T. E. & Jacobs, W. R., Jr. A *Mycobacterium tuberculosis* cytochrome *bd* oxidase mutant is hypersensitive to bedaquiline. *mBio* **5**, e01275–01274, doi: 10.1128/mBio.01275-14 (2014).
62. Jones, S. A. *et al.* Respiration of *Escherichia coli* in the mouse intestine. *Infect. Immun.* **75**, 4891–4899, doi: 10.1128/IAI.00484-07 (2007).
63. Sun, Y. H. *et al.* The small protein *CydX* is required for function of cytochrome *bd* oxidase in *Brucella abortus*. *Front Cell Infect Microbiol* **2**, 47, doi: 10.3389/fcimb.2012.00047 (2012).
64. Garcia, E., Nediaklov, Y. A., Elliott, J., Motin, V. L. & Brubaker, R. R. Molecular characterization of *KatY* (antigen 5), a thermoregulated chromosomally encoded catalase-peroxidase of *Yersinia pestis*. *J. Bacteriol.* **181**, 3114–3122 (1999).
65. Amemura-Maekawa, J., Mishima-Abe, S., Kura, F., Takahashi, T. & Watanabe, H. Identification of a novel periplasmic catalase-peroxidase *KatA* of *Legionella pneumophila*. *FEMS Microbiol. Lett.* **176**, 339–344 (1999).
66. Mehigh, R. J. & Braubaker, R. R. Major stable peptides of *Yersinia pestis* synthesized during the low-calcium response. *Infect. Immun.* **61**, 13–22 (1993).
67. Varnado, C. L., Hertwig, K. M., Thomas, R., Roberts, J. K. & Goodwin, D. C. Properties of a novel periplasmic catalase-peroxidase from *Escherichia coli* O157:H7. *Arch. Biochem. Biophys.* **421**, 166–174 (2004).
68. De Groote, M. A. *et al.* Periplasmic superoxide dismutase protects *Salmonella* from products of phagocyte NADPH-oxidase and nitric oxide synthase. *Proc. Natl. Acad. Sci. USA* **94**, 13997–14001 (1997).
69. Borisov, V. B., Davletshin, A. I. & Konstantinov, A. A. Peroxidase activity of cytochrome *bd* from *Escherichia coli*. *Biochemistry. Biokhimiia* **75**, 428–436 (2010).
70. Borisov, V. B. *et al.* Cytochrome *bd* oxidase from *Escherichia coli* displays high catalase activity: an additional defense against oxidative stress. *FEBS Lett.* **587**, 2214–2218, doi: 10.1016/j.febslet.2013.05.047 (2013).
71. Noble, R. W. & Gibson, Q. H. The reaction of ferrous horseradish peroxidase with hydrogen peroxide. *J. Biol. Chem.* **245**, 2409–2413 (1970).
72. Bekker, M., de Vries, S., Ter Beek, A., Hellingwerf, K. J. & de Mattos, M. J. T. Respiration of *Escherichia coli* Can Be Fully Uncoupled via the Nonelectrogenic Terminal Cytochrome *bd*-II Oxidase. *J. Bacteriol.* **191**, 5510–5517, doi: 10.1128/Jb.00562-09 (2009).
73. Pouvreau, L. A., Strampraad, M. J., Van Berloo, S., Kattenberg, J. H. & de Vries, S. NO, N₂O, and O₂ reaction kinetics: scope and limitations of the Clark electrode. *Methods Enzymol.* **436**, 97–112, doi: 10.1016/S0076-6879(08)36006-6 (2008).
74. VanOrsdel, C. E. *et al.* The *Escherichia coli* *CydX* protein is a member of the *CydAB* cytochrome *bd* oxidase complex and is required for cytochrome *bd* oxidase activity. *J. Bacteriol.* **195**, 3640–3650, doi: 10.1128/JB.00324-13 (2013).
75. Hoese, J., Hong, S., Gehmann, G., Gennis, R. B. & Friedrich, T. Subunit *CydX* of *Escherichia coli* cytochrome *bd* ubiquinol oxidase is essential for assembly and stability of the di-heme active site. *FEBS Lett.* **588**, 1537–1541, doi: 10.1016/j.febslet.2014.03.036 (2014).
76. Chen, H., Luo, Q., Yin, J., Gao, T. & Gao, H. Evidence for the requirement of *CydX* in function but not assembly of the cytochrome *bd* oxidase in *Shewanella oneidensis*. *Biochim. Biophys. Acta* **1850**, 318–328, doi: 10.1016/j.bbagen.2014.10.005 (2015).
77. Lorence, R. M., Miller, M. J., Borochoy, A., Faiman-Weinberg, R. & Gennis, R. B. Effects of pH and detergent on the kinetic and electrochemical properties of the purified cytochrome *d* terminal oxidase complex of *Escherichia coli*. *Biochim. Biophys. Acta* **790**, 148–153 (1984).
78. Borisov, V. B. *et al.* Interaction of the bacterial terminal oxidase cytochrome *bd* with nitric oxide. *FEBS Lett.* **576**, 201–204, doi: 10.1016/j.febslet.2004.09.013 (2004).
79. Ogura, Y. & Yamazaki, I. Steady-state kinetics of the catalase reaction in the presence of cyanide. *J. Biochem.* **94**, 403–408 (1983).
80. Jones, P. & Suggett, A. The catalase-hydrogen peroxide system. Kinetics of catalatic action at high substrate concentrations. *Biochem. J.* **110**, 617–620 (1968).
81. Switala, J. & Loewen, P. C. Diversity of properties among catalases. *Arch. Biochem. Biophys.* **401**, 145–154, doi: 10.1016/S0003-9861(02)00049-8 (2002).
82. Takashima, E., Yamada, H., Yamashita, T., Matsushita, K. & Konishi, K. Recombinant expression and redox properties of triheme *c* membrane-bound quinol peroxidase. *FEMS Microbiol. Lett.* **302**, 52–57, doi: 10.1111/j.1574-6968.2009.01830.x (2010).
83. Yamada, H., Takashima, E. & Konishi, K. Molecular characterization of the membrane-bound quinol peroxidase functionally connected to the respiratory chain. *FEBS J.* **274**, 853–866, doi: 10.1111/j.1742-4658.2006.05637.x (2007).

84. Goldman, B. S., Gabbert, K. K. & Kranz, R. G. The temperature-sensitive growth and survival phenotypes of *Escherichia coli* cydDC and cydAB strains are due to deficiencies in cytochrome bd and are corrected by exogenous catalase and reducing agents. *J. Bacteriol.* **178**, 6348–6351 (1996).
85. Borisov, V. B. *et al.* Aerobic respiratory chain of *Escherichia coli* is not allowed to work in fully uncoupled mode. *Proc. Natl. Acad. Sci. USA* **108**, 17320–17324, doi: 10.1073/pnas.1108217108 (2011).
86. Zhang, J., Barquera, B. & Gennis, R. B. Gene fusions with beta-lactamase show that subunit I of the cytochrome bd quinol oxidase from *E. coli* has nine transmembrane helices with the O₂ reactive site near the periplasmic surface. *FEBS Lett.* **561**, 58–62, doi: 10.1016/S0014-5793(04)00125-5 (2004).
87. Mogi, T., Endou, S., Akimoto, S., Morimoto-Tadokoro, M. & Miyoshi, H. Glutamates 99 and 107 in transmembrane helix III of subunit I of cytochrome bd are critical for binding of the heme b_{595-d} binuclear center and enzyme activity. *Biochemistry* **45**, 15785–15792, doi: 10.1021/bi0615792 (2006).
88. Park, S., You, X. & Imlay, J. A. Substantial DNA damage from submicromolar intracellular hydrogen peroxide detected in Hpx-mutants of *Escherichia coli*. *Proc. Natl. Acad. Sci. USA* **102**, 9317–9322, doi: 10.1073/pnas.0502051102 (2005).
89. Kana, B. D. *et al.* Characterization of the cydAB-encoded cytochrome bd oxidase from *Mycobacterium smegmatis*. *J. Bacteriol.* **183**, 7076–7086, doi: 10.1128/JB.183.24.7076-7086.2001 (2001).
90. Chang, W., Small, D. A., Toghrol, F. & Bentley, W. E. Global transcriptome analysis of *Staphylococcus aureus* response to hydrogen peroxide. *J. Bacteriol.* **188**, 1648–1659, doi: 10.1128/JB.188.4.1648-1659.2006 (2006).
91. Small, J. L. *et al.* Perturbation of cytochrome c maturation reveals adaptability of the respiratory chain in *Mycobacterium tuberculosis*. *mBio* **4**, e00475–00413, doi: 10.1128/mBio.00475-13 (2013).
92. Styrts, B. & Klemperer, M. S. Internal pH of human neutrophil lysosomes. *FEBS Lett.* **149**, 113–116 (1982).

Acknowledgements

The authors want to dedicate this paper to professor Simon de Vries, who unexpectedly passed away in the autumn of 2015 during the process of manuscript preparation. This work was supported by an ECHO grant (711.011.004) from the Netherlands Organization for Scientific Research (NWO) to Simon de Vries and an AFR grant (3945775) from the Fonds National de la Recherche Luxembourg to Jo Hoeser. We thank Shalini Sahebudin, Marc Strampraad and Gaël Brasseur for their technical assistance.

Author Contributions

S.A.-A. and J.H. designed and conducted the experiments and analyzed the results. Y.Y. and M.P. performed the mass spectrometry experiments and analyzed the results. D.B. and T.F. analyzed results and provided expertise. S.A.-A. and S.d.V. wrote the paper with contributions from all coauthors.

Additional Information

Competing financial interests: The authors declare no competing financial interests.

How to cite this article: Al-Attar, S. *et al.* Cytochrome *bd* Displays Significant Quinol Peroxidase Activity. *Sci. Rep.* **6**, 27631; doi: 10.1038/srep27631 (2016).



This work is licensed under a Creative Commons Attribution 4.0 International License. The images or other third party material in this article are included in the article's Creative Commons license, unless indicated otherwise in the credit line; if the material is not included under the Creative Commons license, users will need to obtain permission from the license holder to reproduce the material. To view a copy of this license, visit <http://creativecommons.org/licenses/by/4.0/>